1   **Structured demographic buffering: A framework to explore the environment drivers**

2   **and demographic mechanisms underlying demographic buffering**

3

4   Samuel J L Gascoigne[1,*], Maja Kajin[1,2], Shripad Tuljapurkar[3], Gabriel Silva Santos[4], Aldo

5   Compagnoni[5,6], Ulrich K Steiner[7], Anna C Vinton[1], Harman Jaggi[3], Irem Sepil[1] & Roberto

6   Salguero-Gómez [1,8]

7

8   [1] Department of Biology, South Parks Road, University of Oxford, Oxford, United Kingdom

9   [2] Department of Biology, Biotechnical Faculty, University of Ljubljana, Večna pot 111, 1000

10   Ljubljana, Slovenia

11   [3] Biology Department, Stanford University, Stanford, CA, USA

12   [4] National Institute of the Atlantic Forest (INMA), Santa Teresa, Espírito Santo, Brazil

13   [5] Institute of Biology, Martin Luther University Halle-Wittenburg, Halle (Saale), Germany

14   [6] German Centre for Integrative Biodiversity Research (iDiv) Halle-Jena-Leipzig, Leipzig,

15   Germany

16   [7] Institute of Biology, Freie Universität Berlin, Berlin, Germany

17   [8] National Laboratory for Grassland & Agro-ecosystems, Lanzhou University, China

18

19   * corresponding e-mail: samuel.gascoigne@biology.ox.ac.uk

20

21   Keywords: environmental stochasticity, integral projection models (IPMs), life history

22   strategies, stochastic demography

23

24   Running title: Structured demographic buffering

25

26   Word count: 4,090; Tables: 0; Figures: 4; References: 93

27

28   Statement of authorship: SJLG, IS and RSG conceived and managed the project. SJLG, MK,

29   IS and RSG provided early idea development. SJLG, MK, GS, ST and RSG contributed to

30   early methods development. SJLG coded the simulation, performed the analysis and wrote the

31   first draft with contributions from IS and RSG. Later idea contributions and edits to the

32   manuscript came from ST, AC, UKC, ACV and HJ. All authors contributed significantly to the

33   final manuscript.

34

35   Data accessibility statement: All data and code supporting these results will be made open-

36   access on Zenodo upon publication.

37

38   ORCID identifiers:

Samuel J L Gascoigne: 0000-0002-2984-1810   Ulrich K Steiner: 0000-0002-1778-5989
Maja Kajin: 0000-0001-996-5897   Anna C Vinton: 0000-0002-8279-1736
Shripad Tuljapurkar: 0000-0001-5549-4245   Harman Jaggi: 0000-0002-1563-4917
Gabriel Silva Santos: 0000-0001-7991-8807   Irem Sepil: 0000-0002-3228-5480
Aldo Compagnoni: 0000-0001-8302-7492   Roberto Salguero-Gómez: 0000-0002-6085-4433

39

40   **ABSTRACT** (147 out of 150 words)

41   Environmental stochasticity is a key determinant of population viability. Decades of work

42   exploring how environmental stochasticity influences population dynamics have highlighted

43   the ability of some natural populations to limit the negative effects of environmental

44   stochasticity, one of these strategies being demographic buffering. Whilst various methods

45   exist to quantify demographic buffering, we still do not know which environment factors and

46   demographic characteristics are most responsible for the demographic buffering observed in

47   natural populations. Here, we introduce a framework to quantify the relative effects of three

48   key drivers of demographic buffering: environment components (*e.g.*, temporal autocorrelation

49   and variance), population structure, and demographic rates (*e.g.*, progression and fertility).

50   Using Integral Projection Models, we explore how these drivers impact the demographic

51   buffering abilities of three plant species with different life histories and demonstrate how our

52   approach successfully characterises a population's capacity to demographically buffer against

53   environmental stochasticity in a changing world.

54

55 **INTRODUCTION**

56   Understanding how populations minimise the negative effects of environmental stochasticity

57   is central to ecology and evolution (Sutherland *et al.* 2013). A key prediction of life history

58   theory is that increases in the temporal variance of demographic rates (*e.g.,* rates of progression,

59   stasis, retrogression and fertility) lead to reductions in a population's stochastic growth rate

60   (λ_s) (Tuljapurkar 1982, 1989). In extreme cases, this demographic rate variance can lead to

61   local extinction (May 1973; Saether *et al.* 1998; Lennartsson & Oostermeijer 2001; Bull *et al.*

62   2007; Melbourne & Hastings 2008). Critically, environmental stochasticity, a key driver of

63   demographic rate variance (Jongejans *et al.* 2010), is projected to increase due to climate

64   change (Urban 2015; Bathiany *et al.* 2018; Di Cecco & Gouhier 2018; Masson-Delmotte *et al.*

65   2021). Therefore, understanding the environment drivers and demographic mechanisms

66   influencing the relationship between environmental stochasticity and population dynamics is

67   both important and timely.

68   Three key considerations are needed to relate demographic rate variance to population

69   dynamics. First, there are limits to the amount of variance that demographic rate can exhibit

70   without driving a population to local extinction (Arthreya & Karlin 1971; May 1973). Second,

71   the negative effects of demographic rate variance on population growth are exacerbated when

72   the environment drivers impact the demographic rate(s) of highest importance (*i.e.*, sensitivity)

73   to λ_s. However, the negative effect of demographic rate variance on λ_s can be reduced (or

74   increased) when demographic rates covary negatively (or positively) (Tuljapurkar 1982, 1989),

75   as demographic rates can compensate (amplify) for one another within a timestep. For example,

76   demographic compensation may occur if instances of low adult survival happen concurrently

77   with high adult reproduction, or *vice versa* (Sheth & Angert 2018). Third, environment-vital

78   rate reaction norms can moderate the relationship between demographic rate variance and λ_s

79   (King & Hadfield 2019; Bruijning *et al.* 2020). Following Jensen's inequality (1906), convex

80 (U-shaped) environment-demographic rate reaction norms result in a positive effect of

81 demographic rate variance on λ_s, whereas concave (∩-shaped) reaction norms lead to a

82 negative effect (Drake 2005; Koons *et al.* 2009). These three key considerations regarding the

83 impact of stochastic environments on population dynamics have produced key predictions in

84 life history theory (Tuljapurkar *et al.* 2009; Sæther *et al.* 2013), conservation biology (Foley

85 1994; Higgins *et al.* 2000), and agriculture science (Lande *et al.* 1997; Mack 2000). However,

86 these three considerations alone do not allow us to quantify a population's ability to

87 accommodate demographic rate variance; demographic buffering does.

88   Quantifying demographic buffering in natural populations has been a dynamic area of

89 study in recent decades. The field has moved from regression-based approaches, where the

90 deterministic elasticities (or sensitivities) of demographic rates with respect to λ are regressed

91 against the coefficient of variation (or variance) of demographic rates (Pfister 1998; Morris &

92 Doak 2004; further examples in Hilde *et al.* 2020), to a derivative-based approach that uses the

93 summation of stochastic elasticities of variance, $\sum E_{a_{ij}}^{\sigma^2}$, as a measure of demographic buffering

94 (Santos *et al.* 2023; Wang *et al.* 2023). Despite important insights (*e.g.*, McDonald *et al.* 2017),

95 the regression-based approaches have important limitations, such as being confounded by the

96 life cycle's complexity, the lack of standardized methods (Hilde *et al.* 2020), and difficulty in

97 clear-cut interpretations (see Santos *et al.* 2023 for further details).

98   Using the summation of stochastic elasticities of variance, one can explore the

99 environment drivers and demographic mechanisms behind demographic buffering. This insight

100 is possible because $\sum E_{a_{ij}}^{\sigma^2}$ quantifies the proportional contribution of demographic rate

101 variance to λ_s (Tuljapurkar *et al.* 2003; Haridas & Tuljapurkar 2005) and, consequently,

102 directly quantifies degree of demographic buffering. Whilst researchers have previously used

103 $\sum E_{a_{ij}}^{\sigma^2}$ to quantify demographic buffering (Morris *et al.* 2008; Dalgleish *et al.* 2010), we still

104   do not know how different environment components (*i.e.*, temporal autocorrelation and

105   variance), population structure (*i.e.*, distribution of individuals in a population according to

106   states, such as age, stage and/or size), and different demographic rates (*i.e.*, state-specific

107   transition probabilities or reproductive contributions between time t and $t + 1$) impact $\sum E_{a_{ij}}^{\sigma^2}$.

108   Here, we test the effects of the environment components, population structure and

109   demographic rates on the ability of natural populations to remain demographically buffered.

110   We use environment-explicit stochastic integral projection models (IPMs) (Easterling *et al.*

111   2000; Ellner *et al.* 2016) for three perennial plant species from the PADRINO database (Levin

112   *et al.* 2022) to test two hypotheses. We expect that: (H1) environment autocorrelation and

113   variance will have negative effects on $\sum E_{a_{ij}}^{\sigma^2}$. Specifically, as environments become more

114   variable and positively autocorrelated, populations will become less buffered as predicted by

115   Tuljapurkar's (1982, 1989) small-noise approximation. (H2) Environment autocorrelation and

116   variance influence $\sum E_{a_{ij}}^{\sigma^2}$ via different demographic mechanisms. Specifically, we expect that:

117   (H2a) environment autocorrelation influences $\sum E_{a_{ij}}^{\sigma^2}$ via its impact on population structure. We

118   base this prediction on the fact that the impact of environment autocorrelation on population

119   dynamics can be quantified by the degree to which the sequence of environments shifts the

120   population from its long-term mean stable state structure (Tuljapurkar & Haridas 2006).

121   Briefly, the rationale behind this expectation can be simplified by acknowledging that the

122   commutative property of multiplication that applies to unstructured systems (*e.g.,* $2 \times 1 =$

123   1×2) does not apply to structured systems (*e.g.*, $\mathbf{A} \times \mathbf{B} \neq \mathbf{B} \times \mathbf{A}$, where $\mathbf{A}$ and $\mathbf{B}$ are matrices

124   of size $> 1 \times 1$). In turn, since the structure of the population is encoded into the population

125   state distributions, we hypothesize that the impact of environment autocorrelation on $\sum E_{a_{ij}}^{\sigma^2}$ is

126   strongly mediated by population structure. Similarly, we expect (H2b) environment variance

127   to influence $\sum E_{a_{ij}}^{\sigma^2}$ via the populations' underlying demographic rates. This prediction also

128   follows Tuljapurkar's small-noise approximation (1982, 1989), where the impact of

129   environment variance can be approximated by the summed product of the variance and

130   sensitivities of individual demographic rates.

131

132   **METHODS**

133   <u>Stochastic integral projection models</u>

134   To explore the drivers of demographic buffering, we used integral projection models (IPMs).

135   IPMs are discrete time population models (*i.e.*, they project populations are projected across

136   well-defined intervals of time from t to $t + 1$) that are structured with respect to a continuous

137   variable (*e.g.*, height, length, mass; Easterling *et al.* 2000; Ellner *et al.* 2016). To investigate

138   the environment drivers and demographic mechanisms that impact degrees of demographic

139   buffering in natural populations, we used environment explicit, parameter-stochastic IPMs for

140   the *Berberis thunbergii* (Japanese barberry; Merow *et al.* 2017), *Calathea crotalifera*

141   (rattlesnake plant; Westerband & Horvitz 2017) and *Heliconia tortuosa* (red twist Heliconia;

142   Westerband & Horvitz 2017), extracted from the PADRINO IPM database (Levin et al. 2022).

143   The chosen model structure allows us to individually influence regression parameters that

144   underpin the IPM subkernels (*i.e.*, the survival **P**- and fertility **F**-subkernels) based on the

145   environment conditions to test our hypotheses.

146   We chose these three published IPMs to compare the roles of environment parameters

147   and λ_s on $\sum E_{a_{ij}}^{\sigma^2}$ to gain some generality. The *B. thunbergii* IPM uses five environment

148   parameters to build its kernels: mean temperature during warmest month, mean May

149   precipitation, photosynthetically active radiation (PAR), soil nitrogen, and soil pH. The *C.*

150   *crotalifera* and *H. tortuosa* IPMs use two environment parameters to define their kernels:

151   canopy openness and photosynthetic rate. The kernel structure and parameters used in vital rate

152 regressions for *B. thunbergii*, *C. crotalifera* and *H. tortuosa* are detailed in supplementary

153 tables 1, 2 and 3, respectively. Furthermore, the models inhabit different domains of λ_s. The

154 models of *B. thunbergii* and *H. torutosa* have values of $\lambda_s > 1$ (*B. thunbergii*: $\lambda_s = 1.378$; *H.*

155 *tortuosa*: $\lambda_s = 1.367$), implying long-term population growth, *C. crotalifera* has a $\lambda_s < 1$ (λ_s

156 = 0.976), describing long-term population decline (Figure S1). Since *C. crotalifera* and *H.*

157 *torutosa* have the same environment parameters and *B. thunbergii* and *H. tortuosa* have similar

158 λ_s values, by comparing demographic buffering across these species, we aim to examine

159 possible impacts of environment parameters and λ_s on $\sum E_{a_{ij}}^{\sigma^2}$ across the autocorrelation –

160 proportional variance parameter space.

161 <u>Simulation methodology</u>

162 To explore the roles of (H1) environment drivers as well as (H2a) population structure and

163 (H2b) demographic rates on demographic buffering, we simulated IPMs across the

164 environment autocorrelation – variance parameter space. In this simulation, all combinations

165 of stochastic environment parameters, with autocorrelation ranging from -0.8 to 0.8 and

166 proportional variance ranging from 0.9 (10% less variance in the environment than the IPM in

167 PADRINO) to 1.1 (10% more variance in the environment that the IPM in PADRINO) were

168 generated for all environment parameters. *B. thunbergii* had five environment parameters,

169 whilst *C. crotalifera* and *H. tortuosa* had two environment parameters (Fig. 1a,b). We used

170 these sequences of environment parameters to construct the time series of 1,000 IPM kernels

171 from which we then estimated λ_s (eq. 1). Specifically, to calculate λ_s: (1) a population of

172 random structure was initialized, whereby the proportion of individuals of a given size class

173 was generated from a uniform distribution ranging between the upper and lower limits of the

174 IPMs (see Tables S1-3), (2) the population was then multiplied through the series of 1,000

175   parameter-stochastic IPM kernels, and (3) population sizes from timestep 200 to 1,000 were

176   used to calculate λ_s following the equation:

177   (Eq. 1) $\lambda_s = \exp\left(E\left[\ln\left(\frac{N_{t+1}}{N_t}\right)\right]\right).$

178   We omitted the first 200 projections from our calculation of λ_s to discard transient dynamics

179   effects on short-term population size distributions (McDonald *et al.* 2016).

180   <u>Generating environment time series</u>

181   To explore the environment drivers of demographic buffering (H1), we manipulated the

182   temporal autocorrelation and variance of environmental variables in our environmentally

183   explicit stochastic IPMs. Whilst the effects of variance of demographic rates on population

184   dynamics are commonly researched in population ecology (*e.g.*, Jackson *et al.* 2022; Le Coeur

185   *et al.* 2022), temporal autocorrelation is much less explored despite temporal autocorrelation

186   having broad impacts on population dynamics (Petchey *et al.* 1997; Petchey 2000; Smallegange

187   *et al.* 2014; Evers *et al.* 2023), life histories (Paniw *et al.* 2018; Vinton *et al.* 2023) and

188   evolution (Wieczynski *et al.* 2018; Vinton *et al.* 2022). To fill this gap in knowledge, we used

189   a first-order autoregressive function to generate the sequence of environment values used to

190   build the series of IPM kernels. Here, φ represents the degree of autocorrelation across time

191   steps whilst, ϵ_{t+1} represents white noise (*i.e.*, random draws from a normal distribution,

192    $\boldsymbol{\epsilon} \sim N(0,1)$).

193   (Eq. 2) $X_{t+1} = \varphi X_t + \epsilon_{t+1}$

194   Subsequently, to coerce the autocorrelated series (**X**) to realistic values for the vital rate

195   regressions that build the IPMs (shown in Tables S1-3), the final sequence of environment

196   values was to a desired mean (μ) and variance (σ^2) of the simulated environment:

197 (Eq. 3) $\text{environment} = \left[\dfrac{\sqrt{\sigma^2}[\mathbf{X} - \text{mean}(\mathbf{X})]}{\sqrt{\text{var}(\mathbf{X})}} \right] + \mu$

198 As our objective is not to evaluate the effect of shifts in mean environment values on

199 demographic buffering but rather to examine the impacts of variance and autocorrelation, μ

200 values were kept constant across simulations, whilst σ^2 values varied across simulations.

201 Since the environment variables across the three species have different variances ($\sigma^2_{init.}$), to

202 standardize the increase/decrease in environment variance across parameters, we manipulated

203 variances proportional to their variances coded in the PADRINO database ($\sigma^2_{prop.}$) (Levin *et*

204 *al.* 2022).

205 (Eq. 4) $\sigma^2 = \sigma^2_{init.}\sigma^2_{prop.}$

206 <u>Analysing the effects of environment autocorrelation and variance</u>

207 To explore the effects of environmental components on each species' ability to remain

208 demographically buffered (H1,2), we constructed a suite of linear models using autocorrelation

209 and proportional variance as predictors whilst also including an autocorrelation × proportional

210 variance as an interaction term. Furthermore, since the impact of autocorrelation and

211 proportional variance on demographic buffering may be nonlinear, we also constructed models

212 using the quadratic and cubic forms of proportional variance and autocorrelation as predictors.

213 To select the most appropriate model to describe the data, we used model comparison based on

214 AIC (see supplementary materials p. 4 for the full analysis pipeline and Tables S4-12 for full

215 AIC break down). After selecting the most parsimonious model, we calculated the proportion

216 of variance in $\sum E^{\sigma^2}_{a_{ij}}$ that can be explained by the summed contributions of autocorrelation,

217 proportional variance, autocorrelation × proportional variance and residuals (Figure 1c).

218

219   <u>Perturbation analyses to quantify $\sum E_{a_{ij}}^{\sigma^2}$</u>

220   To quantify the degree of demographic buffering across our simulations (testing H1,2), we

221   calculated the summation of stochastic elasticities of variance of demographic rates with

222   respect to λ_s. We estimated this variable, $\sum E_{a_{ij}}^{\sigma^2}$, *numerically*. Whilst the **K**-kernel of an IPM

223   is defined as a continuous map that projects a continuously structured population across time

224   steps, in practice we discretise the kernel into a matrix notated as **A** (Easterling *et al.* 2000;

225   Ellner *et al.* 2016). Since **A** is composed of individual matrix elements (a_{ij}) and our stochastic

226   environment generates a temporal sequence of **A** matrices, we can quantify the temporal

227   variance of each a_{ij} element in matrix **A**. In turn, we numerically calculate $\sum E_{a_{ij}}^{\sigma^2}$ by perturbing

228   the temporal variance of each matrix element (a_{ij}) from our IPMs individually by 0.00001

229   proportionate (elasticity) to the unperturbed temporal variance of that matrix element. After

230   perturbation of the matrix element, we calculated a perturbed stochastic population growth rate

231    $\left(\lambda_s^{*a_{ij}} \right)$. The summation of these weighted differences in λ_s and $\lambda_s^{*a_{ij}}$ yields $\sum E_{a_{ij}}^{\sigma^2}$.

232   (Eq. 5) $\sum E_{a_{ij}}^{\sigma^2} = \sum \left[\frac{\text{var}(a_{ij})}{\lambda_s} * \frac{\lambda_s^{*a_{ij}} - \lambda_s}{0.00001 * \text{var}(a_{ij})} \right]$

233   To calculate the impact of demographic rates on demographic buffering (H2b), we perturbed

234   the subkernels that describe survival-dependent changes in size (**P**) and fertility (**F**) using the

235   same method we used for the **K**-kernels. After calculating the subkernel-level elasticities of

236   variance (Griffith 2017), we subtracted the subkernel summed elasticities of demographic rates

237   to calculate their relative contributions: **P** – **F** contribution. Positive (negative) values of **P** – **F**

238   contribution indicate relative variance in rates of survival-dependent changes in size are more

239   (less) impactful on λ_s than relative variance in rates of fertility.

240   <u>Quantifying the impact of population structure on $\sum E_{a_{ij}}^{\sigma^2}$</u>

241 To analyse how population structure influences demographic buffering (H2a), we used two

242 numerical approaches. Whilst methods exist to *analytically* measure the impact of population

243 structure on asymptotic properties of population dynamics (Tuljapurkar & Lee 1997), currently

244 there are no analytical approaches to quantify the degree to which multiple environment

245 components influence $\sum E_{a_{ij}}^{\sigma^2}$ via population structure. In turn, we use two measures of

246 population structure using a *regression-based approach* and an *estimate-based approach.*

247 These approaches *numerically* link the impact of environment autocorrelation and variance on

248 $\sum E_{a_{ij}}^{\sigma^2}$ via population structure. Importantly, using these two approaches to investigate H2a

249 allows us to cross-validate outputs (*i.e.*, the hypothesized result of environment autocorrelation

250 impacting $\sum E_{a_{ij}}^{\sigma^2}$ via shifts in population structure).

251 The *regression-based approach* involved examining deviances from stationary

252 distributions. To do so, we regressed the scaled values – relative to the average size distribution

253 – of the expected mean buffering value of a randomly selected individual in the population

254 ($\sum E_{a_{ij}}^{\sigma^2}$ |ASD) against scaled values of $\sum E_{a_{ij}}^{\sigma^2}$. Deviances of $\sum E_{a_{ij}}^{\sigma^2}$ |ASD$\sim \sum E_{a_{ij}}^{\sigma^2}$ from a 1-to-1

255 line (*i.e.*, the existence of residuals from this regression) indicates shifts in population structure

256 may be influencing $\sum E_{a_{ij}}^{\sigma^2}$. Subsequently, regressing these residuals against the environment

257 components allows us to implicate an environment component – hypothesized to be

258 environment autocorrelation [H2a] – as driving the impact of population structure on $\sum E_{a_{ij}}^{\sigma^2}$.

259 To perform this approach, we weighted $\sum E_{a_{ij}}^{\sigma^2}$ by the average size distribution (*i.e.*, the average

260 size distribution [ASD] of individuals in the population across the simulation) to calculate

261 $\sum E_{a_{ij}}^{\sigma^2}$ |ASD. To determine the population's average size distribution for a given environment,

262 we iterated 1,000 randomly generated size distributions through the series of stochastic kernels

263 and retained the mean of all size distributions across time steps 200 to 1,000 as an estimation

264   of the average size distribution. Burning in the first 200 timesteps mitigates the impact of

265   transients on the ASD. After calculating $\sum E_{a_{ij}}^{\sigma^2}$|ASD, the emergent distribution was z-

266   transformed (mean = 0, standard deviation = 1) and regressed against z-transformed values of

267     $\sum E_{a_{ij}}^{\sigma^2}$ not informed by the average size distribution. Residuals from this regression represent

268   a possible impact of population structure on $\sum E_{a_{ij}}^{\sigma^2}$. To further investigate the impact of

269   environment autocorrelation and variance on $\sum E_{a_{ij}}^{\sigma^2}$ via said residuals, we modelled the

270   residuals of the $\sum E_{a_{ij}}^{\sigma^2}$|ASD $\sim \sum E_{a_{ij}}^{\sigma^2}$ regression in response to environment autocorrelation and

271   variance.

272   The *estimate-based approach* involved calculating the mean of the distribution of

273   demographic buffering across a life history, termed *mean buffered size*. Calculating mean

274   buffered size allows us to explore if the degree of buffering across a life history is shifted

275   towards smaller or larger sizes across the environment autocorrelation – variance parameter

276   space. To calculate this mean buffered size, we calculated the relative size (*i.e.*, 0 = smallest

277   possible size (α) and 1 = maximum possible size (ω)) that corresponds to the centre of the

278   distribution of $\sum E_{a_{ij}}^{\sigma^2}$ across the domain of sizes (Eq. 6). This calculation mirrors the method

279   of calculating generation time as the mean age of reproductive individuals in the population

280   (Ebert 1999, pg. 14).

281   (Eq. 6) $mean\ buffered\ size\ = \frac{1}{\omega}\left[\frac{\sum_j\left[j\sum_i E_{a_{ij}}^{\sigma^2}\right]}{\sum E_{a_{ij}}^{\sigma^2}} - \alpha\right]$

282   After calculating the mean buffered size for each species across the environment

283   autocorrelation – variance parameter space, we regressed mean buffered size against the

284   environment components to test our hypothesis that environment autocorrelation influences

285     $\sum E_{a_{ij}}^{\sigma^2}$ via shifts in population structure (H2a).

286

RESULTS

<u>Testing H1: Environment variance is the primary driver of demographic buffering</u>

Here we tested the hypothesis that environment autocorrelation and variance have negative effects on demographic buffering as quantified via $\sum E_{a_{ij}}^{\sigma^2}$ (H1). To do so, we ran simulations of the *Berberis thunbergii*, *Calathea crotalifera* and *Heliconia tortuosa* IPMs across the domain of autocorrelation and proportional variance values and calculated $\sum E_{a_{ij}}^{\sigma^2}$. We found environment variance to be the primary driver of variance in $\sum E_{a_{ij}}^{\sigma^2}$ (Figure 2). The summed contributions of proportional variance accounted for 94% of the variance of $\sum E_{a_{ij}}^{\sigma^2}$ in *B. thunbergii* ($R^2 = 0.99$, Table S4) (Figure 2a), 85% of the variance of $\sum E_{a_{ij}}^{\sigma^2}$ in *C. crotalifera* ($R^2 = 0.89$, Table S5 (Figure 2b) and 83% of the variance of $\sum E_{a_{ij}}^{\sigma^2}$ in *H. tortuosa* ($R^2 = 0.89$, Table S6) (Figure 2c). Supporting our hypothesis, environment variance had a negative effect on $\sum E_{a_{ij}}^{\sigma^2}$ (see models for *B. thunbergii*, *C. crotalifera*, and *H. tortuosa* in Tables S4-6). However, we did not find evidence for a negative effect of environment autocorrelation on $\sum E_{a_{ij}}^{\sigma^2}$. Instead, all species were best modelled when the quadratic and cubic forms of autocorrelation were used as predictors of $\sum E_{a_{ij}}^{\sigma^2}$ without the inclusion of a linear effect of autocorrelation. This finding indicates the impact of autocorrelation on $\sum E_{a_{ij}}^{\sigma^2}$ is non-linear across the environment autocorrelation and variance parameter space.

<u>Testing H2a: Temporal autocorrelation influences demographic buffering via population structure</u>

We used two approaches to test the hypothesis that temporal autocorrelation influences demographic buffering via shifts in population structure (H2a). First, we used a measure of

308   demographic buffering that accounts for population structure ($\sum E_{a_{ij}}^{\sigma^2}$ |ASD) and regressed that

309   against our normal measure of demographic buffering ($\sum E_{a_{ij}}^{\sigma^2}$). Second, we measured the shifts

310   in the distribution of buffering across the life history in response to environment components.

311   In our first approach, we regressed scaled values of $\sum E_{a_{ij}}^{\sigma^2}$ across all simulations

312   against their respective $\sum E_{a_{ij}}^{\sigma^2}$ normalized by simulation specific stable size distribution

313   ($\sum E_{a_{ij}}^{\sigma^2}$ |ASD). Since both values are scaled to mean = 0 with standard deviation = 1, any

314   deviation of $\sum E_{a_{ij}}^{\sigma^2}$ |ASD $\sim \sum E_{a_{ij}}^{\sigma^2}$ from the 1-to-1 regression line indicates temporal shifts in

315   population structure may impact demographic buffering. Interestingly, we found heterogeneity

316   in the degree to which $\sum E_{a_{ij}}^{\sigma^2}$ |ASD differed from $\sum E_{a_{ij}}^{\sigma^2}$ across species. Whilst *C. crotalifera*

317   reported a 1-to-1 regression line between $\sum E_{a_{ij}}^{\sigma^2}$ |ASD and $\sum E_{a_{ij}}^{\sigma^2}$ (R^2 = 1, Figure 3d), *B.*

318   *thunbergii* and *H. tortuosa* had residuals (*B. thunbergii*: R^2 = 0.9977, Fig. 3a; *H. tortuosa*: R^2

319   = 0.9995, Figure 3g). These residuals indicate that population structure may influence $\sum E_{a_{ij}}^{\sigma^2}$,

320   specifically in *B. thunbergii* and *H. tortuosa*.

321   To determine if environment autocorrelation is driving these residuals, we modelled the

322   residuals of the $\sum E_{a_{ij}}^{\sigma^2}$ |ASD $\sim \sum E_{a_{ij}}^{\sigma^2}$ regression against environment autocorrelation and

323   variance. Supporting our hypothesis (H2a), we found the residuals of the $\sum E_{a_{ij}}^{\sigma^2}$ |ASD $\sim \sum E_{a_{ij}}^{\sigma^2}$

324   regression are mostly explained by environment autocorrelation (Figures 3b,e,h). In *B.*

325   *thunbergii* and *H. tortuosa* (the species with the largest residuals from the $\sum E_{a_{ij}}^{\sigma^2}$ |ASD $\sim \sum E_{a_{ij}}^{\sigma^2}$

326   regression), environment autocorrelation accounted for 48% (R^2 = 0.56, Figure 3b, Table S7)

327   and 46% (R^2 = 0.84, Figure 3h, Table S9) of the variance in residuals respectively; whilst

328   environment variance only accounted for 2% of the variance in residuals in both species.

329   Regarding *C. crotalifera*, the largest contributor to variance in residuals was unexplained

330   residual variance (56%, R^2 = 0.47, Figure 3e, Table S8), followed by environment

331   autocorrelation (28%) and variance (16%).

332   In our second approach, we analysed the impact of environment autocorrelation and

333   variance on the distribution of demographic buffering across a life cycle. In turn, we calculated

334   the centre of the distribution of demographic buffering across a life history: mean buffered size.

335   Echoing the findings from the first line of enquiry, mean buffered size was best explained by

336   changes in environment autocorrelation – especially in *B. thunbergii* and *H. tortuosa*.

337   Specifically, in *B. thunbergii*, 73% of the variance in mean buffered size was attributed to

338   environment autocorrelation whilst 17% was attributed to environment variance (R^2 = 0.91,

339   Figure 3c, Table S10). Additionally, in *H. tortuosa*, 91% of the variance in mean buffered size

340   was attributed to environment autocorrelation with only 0.1% being attributed to changes in

341   environment variance (R^2 = 0.97, Figure 3i, Table S12). And finally, just as in the first line of

342   enquiry, $\sum E_{a_{ij}}^{\sigma^2}$ in *C. crotalifera* is less exposed to impacts of shifts in population structure as

343   the distribution of mean buffered size across the environment autocorrelation – variance

344   parameter space was mostly explained by residual variance (78%) rather than environment

345   autocorrelation (17%) or environment variance (5%) (R^2 = 0.26, Figure 3f, Table S11).

346

347   <u>Testing H2b: Demographic buffering is most sensitive to environment variance's impact on</u>

348   <u>rates of progression</u>

349   To test the hypothesis that environment variance impacts demographic buffering through vital

350   rates (H2b), we ran the same perturbation analysis used to calculate $\sum E_{a_{ij}}^{\sigma^2}$ at the level of the

351   sub-kernels: **P**-subkernel (survival-dependent changes in size) and the **F**-subkernel (fertility).

352   By taking the difference of the subkernel elasticities of variance (*i.e.*, **P** – **F** contribution), we

353   investigated (1) the role of underlying rates on demographic buffering and (2) the

354   environmental components that influence the **P – F** contribution across the environment

355   autocorrelation – variance parameter space.

356   First, we determined if the **P – F** contribution is a sufficient predictor of $\sum E_{a_{ij}}^{\sigma^2}$. The **P**

357   **– F** contribution was highly predictive of $\sum E_{a_{ij}}^{\sigma^2}$ across all species (Figure 4a). *B. thunbergii*

358   had a negative relationship between **P – F** contribution and $\sum E_{a_{ij}}^{\sigma^2}$ ($r(223) = -0.968$, $p<0.001$),

359   whilst *C. crotalifera* and *H. tortuosa* had positive relationships (*C. crotalifera*: $r(223) = 0.999$,

360    $p<0.001$; *H. tortuosa*: $r(223) = 0.983$, $p<0.001$). These results indicate lower degrees of

361   demographic buffering are associated with a greater impact of variance in rates of progression

362   (*vs.* fertility) in *B. thunbergii*, but the opposite, a greater impact of variance in fertility (*vs.*

363   progression) in *C. crotalifera* and *H. tortuosa*.

364   To test if variance in **P – F** contribution is most explained by environment variance

365   rather than autocorrelation (H2b), we regressed **P – F** contribution against the environment

366   components. Across the three species, the **P – F** contribution was mostly explained by

367   differences in degrees of environment variance rather than autocorrelation across the

368   environment autocorrelation – variance parameter space (Figures 4b-d). Specifically,

369   environment variance explained 80%, 85% and 86% of the variance of **P – F** contribution in

370   *B. thunbergii* ($R^2 = 0.99$, Figure 4b, Table S13), *C. crotalifera* ($R^2 = 0.89$, Figure 4c, Table

371   S14) and *H. tortuosa* ($R^2 = 0.89$, Figure 4d, Table S15), respectively. However, of the

372   remaining variance, environment autocorrelation explained 17%, 3% and 2% of the variance

373   of **P – F** contribution, respectively.

374

375   **DISCUSSION**

376 Environment drivers and demographic mechanisms are key to quantify and predict a

377 population's capacity for demographic buffering. Using three stochastic IPMs from the

378 PADRINO database (Levin *et al.* 2022), we obtain partial support for the hypothesis that

379 environment autocorrelation and variance negatively impact a population's capacity to remain

380 demographically buffered (H1). Interestingly, whilst environment variance negatively affects

381 demographic buffering, there is a nonlinear effect of temporal autocorrelation on demographic

382 buffering. Furthermore, even though environment autocorrelation and variance combine to

383 make the environment time series, we show that their effects on demographic buffering are

384 orthogonal dimensions of environmental stochasticity. Indeed, the effect of temporal

385 autocorrelation on demographic buffering ($\sum E_{a_{ij}}^{\sigma^2}$) is mediated by population structure (H2a),

386 whilst the effect of environment variance on $\sum E_{a_{ij}}^{\sigma^2}$ is mediated by underlying demographic

387 rates (H2b). Specifically, the influence of environment variance on rates of progression *vs.*

388 fertility is the greatest driver of differences in $\sum E_{a_{ij}}^{\sigma^2}$ across variable environments in the three

389 examined species. This finding builds on multiple lines of evidence showing how different life

390 histories can persist in variable environments via the differential variance of progression *vs.*

391 fertility rates (Gaillard *et al.* 1998; Pfister 1998).

392   Identifying the mechanisms that underpin the ability of natural populations to buffer

393 against environmental stochasticity offers a powerful framework to explore a population's

394 vulnerability to climate change. Current climatic forecasts predict environmental stochasticity

395 to increase with global climate change (Masson-Delmotte *et al.* 2021). For example, periods of

396 extreme variation in temperature and precipitation are expected to increase in the tropics and

397 sub-tropics which host the highest biodiversity (temperature: Bathiany *et al.* 2018;

398 precipitation: Trenberth 2011). Furthermore, extreme weather events are expected to become

399 more common, leading to increased autocorrelation (*e.g.*, tropical cyclones: Knutson *et al.*

400 2010; fire frequency: Halofsky *et al.* 2020). However, not all environmental components affect

401 populations the same way (Hoffmann & Bridle 2022; Vinton *et al.* 2022, 2023). The shape of

402 demographic rates across a life history varies widely across the tree of life (Jones *et al.* 2014;

403 Salguero-Gómez *et al.* 2017; Paniw *et al.* 2018; Healy *et al.* 2019; Varas-Enriquez *et al.* 2022).

404 Therefore, predicting the susceptibility of populations to environmental stochasticity, without

405 a regard to the mechanism, overlooks key heterogeneity in the demographic processes

406 necessary for accurate predictions. Our framework provides a promising avenue to incorporate

407 this heterogeneity for informed analyses of the role of environmental stochasticity in a

408 population's demographic buffering capacity.

409 Our results highlight an interesting, but often overlooked, role of population structure

410 in demographic buffering. Whilst we find environment autocorrelation to primarily impact

411 demographic buffering via shifts in population structure, there is also species-level

412 heterogeneity in the strength and direction by which environment autocorrelation shifts

413 population structure. Furthermore, our results indicate portions of the heterogeneity in $\sum E_{a_{ij}}^{\sigma^2}$

414 are explained by the interaction between environment autocorrelation and variance. One likely

415 source of this heterogeneity is transient dynamics (*i.e.*, short-term, progressively weakening

416 realizations of non-asymptotic lambda values resulting from a population not being at its stable-

417 stage distribution (Stott *et al.* 2011)). Whilst transient dynamics represent a suite of different

418 stereotyped population dynamics (Capdevila *et al.* 2020), only *reactivity* (the degree to which

419 a population not at its stable-stage distribution increases/decreases relative to that same

420 population projected from its stable-stage distribution (Neubert & Caswell 1997)) has been

421 linked to stochastic demography (McDonald *et al.* 2016). However, the link between reactivity,

422 along with other transient dynamics, and demographic buffering remains unknown. Future

423 work analysing which transient dynamics are increasing and decreasing levels of demographic

424 buffering will finally integrate the analysis of transient dynamics with stochastic demography.

425   Historically, studies of life histories in stochastic environments have followed two

426   branches: modelling and dimension reduction. Modelling life histories in stochastic

427   environments, whereby analytic or numeric methods are used for demographic inference in

428   individual populations, has progressively put to rest some key problems within life history

429   theory (iteroparity: Orzack & Tuljapurkar 1989; Tuljapurkar *et al.* 2009; diapause: Tuljapurkar

430   & Istock 1993; migration: Wiener & Tuljapurkar 1994; biennialism: Klinkhammer & de Jong

431   1983; Roerdink 1988, 1989; homeostasis: Orzack 1985; lability: Koons *et al.* 2009; Jongejans

432   *et al.* 2010; Barraquand & Yoccoz 2013; summarized in Caswell (2001, pg. 440)). However,

433   one of the limitations of a modelling approach is losing the realism captured within constraints,

434   phylogenetic history or selection gradients that drive variance patterns in demographic rates.

435   From the empirical side, researchers have used dimension reduction techniques to

436   unmask the patterns life histories exhibit in variable environments. Dimension reduction

437   techniques, such as phylogenetically controlled principal component analyses (Revell 2012),

438   are especially useful as a life history is not a value nor an object; a life history strategy is an

439   abstract concept that researchers probe with life history traits – such as: longevity, age at

440   maturity, average body size, *etc*. To capture the signal of an individual life history strategy

441   through the dimensionality, reducing the multidimensionality of life history metrics to its most

442   important axes of variance (*i.e.*, principal components) has led to key discoveries (two-axes of

443   life history variance: Salguero-Gómez *et al.* 2017; Healy *et al.* 2019). Furthermore, this

444   approach has been used to model life histories in stochastic environments (Paniw *et al.* 2018;

445   Romeijn & Smallegange 2022). However, this approach is limited to modelling only one

446   component of a variable environment (*e.g.,* environment autocorrelation *or* variance). This

447   limitation is further emphasized by our results showing non-linearities between the effects of

448   environmental components on $\sum E_{a_{ij}}^{\sigma^2}$, thereby illustrating that the impact of an environment

449   component on demographic process is context dependent.

450   Using our framework, researchers can stitch the modelling and dimension reduction

451   approaches together. Our framework can be applied to any environmentally explicit structured

452   population models: from physiologically structured population models (de Roos 1997) to

453   matrix population models (Caswell 2001) to integral projection models (Easterling *et al.* 2000;

454   Ellner *et al.* 2016), to dynamic energy budget models (Nisbet *et al.* 2000; Smallegange *et al.*

455   2017). By using open-access data (COMPADRE: Salguero-Gómez *et al.* 2015; COMADRE:

456   Salguero-Gómez *et al.* 2016; PADRINO: Levin *et al.* 2022; AmP: Marques *et al.* 2018),

457   researchers can explore the combined impact of autocorrelation and variance on $\sum E_{a_{ij}}^{\sigma^2}$ by

458   interfacing the time series of a structured population models with stochastic matrices (as in

459   Paniw *et al.* 2018). Once the landscape of $\sum E_{a_{ij}}^{\sigma^2}$ is mapped across environment autocorrelation

460   and variance, the relative contributions of constraints, phylogeny and species-specific effects

461   on $\sum E_{a_{ij}}^{\sigma^2}$ will be realized. This combined approach of modelling and dimension reduction

462   offers generalization in a previously exception driven area of life history theory.

463   In conclusion, structure matters. Since Leslie (1945) and Lefkovitch (1965),

464   demographers have explored how relatively simple structured population models can be used

465   for biological inference. From transient dynamics (Hastings 2001; Ezard *et al.* 2010; Capdevila

466   *et al.* 2020, 2022), to structured Lotka-Volterra models (de Roos *et al.* 1990; de Roos 2021) to

467   stability analysis (Cushing *et al.* 2003), researchers have generated a rich body of theory and

468   evidence for the impact of population structure on demographic inferences. However, the

469   impact of environment structure, in the form of individual climate drivers (*e.g.*, temporal

470   autocorrelation and variance), and their corresponding demographic mechanisms that mediate

471   their effects are uncoupled. We argue they should be stitched together. Our framework

472   exploring demographic buffering across the environment autocorrelation – variance parameter

473 space joins a recent push stitching the impacts of climate drivers (*e.g.*, Vinton *et al.* 2022) with

474 their respective demographic mechanisms (*e.g.*, Le Coeur *et al.* 2022).

475

487

488

REFERENCES

Arthreya, K.B. & Karlin, S. (1971). On branching processes with random environments: I: Extinction probabilities. *Ann. Math. Stat.*, 42, 1499–1520.

Barraquand, F. & Yoccoz, N.G. (2013). When can environmental variability benefit population growth? Counterintuitive effects of nonlinearities in vital rates. *Theor. Popul. Biol.*, 89, 1–11.

Bathiany, S., Dakos, V., Scheffer, M. & Lenton, T.M. (2018). Climate models predict increasing temperature variability in poor countries. *Sci. Adv.*, 4, 1–11.

Bruijning, M., Metcalf, C.J.E., Jongejans, E. & Ayroles, J.F. (2020). The Evolution of Variance Control. *Trends Ecol. Evol.*, 35, 22–33.

Bull, J.C., Pickup, N.J., Pickett, B., Hassell, M.P. & Bonsall, M.B. (2007). Metapopulation extinction risk is increased by environmental stochasticity and assemblage complexity. *Proc. R. Soc. B Biol. Sci.*, 274, 87–96.

Capdevila, P., Stott, I., Beger, M. & Salguero-Gómez, R. (2020). Towards a Comparative Framework of Demographic Resilience. *Trends Ecol. Evol.*, 35, 776–786.

Capdevila, P., Stott, I., Cant, J., Beger, M., Rowlands, G., Grace, M., *et al.* (2022). Life history mediates the trade-offs among different components of demographic resilience. *Ecol. Lett.*, 25, 1566–1579.

Caswell, H. (2001). *Matrix population models: Construction, analysis, and interpretation*. 2nd editio. Sinauer, Sunderland, MA.

Di Cecco, G.J. & Gouhier, T.C. (2018). Increased spatial and temporal autocorrelation of temperature under climate change. *Sci. Rep.*, 8, 1–9.

Le Coeur, C., Yoccoz, N.G., Salguero-Gómez, R. & Vindenes, Y. (2022). Life history adaptations to fluctuating environments : Combined effects of demographic buffering and lability of demographic parameters. *Ecol. Lett.*, 1–13.

Cushing, J.M., Constantino, R.F., Dennis, B., Desharnais, R. & Henson, S.M. (2003). *Chaos in ecology: experimental nonlinear dynamics*. Elsevier.

Dalgleish, H.J., Koons, D.N. & Adler, P.B. (2010). Can life-history traits predict the response of forb populations to changes in climate variability? *J. Ecol.*, 98, 209–217.

Drake, J.M. (2005). Population effects of increased climate variation. *Proc. R. Soc. B Biol. Sci.*, 272, 1823–1827.

Easterling, M.R., Ellner, S.P. & Dixon, P.M. (2000). Size-specific sensitivity: Applying a new structured population model. *Ecology*, 81, 694–708.

Ebert, T.A. (1999). Populations Methods in Demography. *Methods &Demography*.

Ellner, S.P., Childs, D.Z. & Rees, M. (2016). *Data-driven Modelling of Structured Populations*.

Evers, S.M., Knight, T.M. & Compagnoni, A. (2023). The inclusion of immediate and lagged climate responses amplifies the effect of climate autocorrelation on long-term growth rate of populations. *J. Ecol.*, 1–12.

528 Ezard, T.H.G., Bullock, J.M., Dalgleish, H.J., Millon, A., Pelletier, F., Ozgul, A., *et al.*
529   (2010). Matrix models for a changeable world: The importance of transient dynamics in
530   population management. *J. Appl. Ecol.*, 47, 515–523.

531 Foley, P. (1994). Predicting Extinction Times from Environmental Stochasticity and Carrying
532   Capacity. *Conserv. Biol.*, 8, 124–137.

533 Gaillard, J.-M., Festa-Bianchet, M. & Yoccoz, N.G. (1998). Population dynamics of large
534   herbivores: variable recruitment with constant adult survival. *Trends Ecol. Evol.*, 13,
535   249–251.

536 Griffith, A.B. (2017). Perturbation approaches for integral projection models. *Oikos*, 126,
537   1675–1686.

538 Halofsky, J.E., Peterson, D.L. & Harvey, B.J. (2020). Changing wildfire, changing forests:
539   the effects of climate change on fire regimes and vegetation in the Pacific Northwest,
540   USA. *Fire Ecol.*, 16.

541 Haridas, C. V. & Tuljapurkar, S. (2005). Elasticities in variable environments: Properties and
542   implications. *Am. Nat.*, 166, 481–495.

543 Hastings, A. (2001). Transient dynamics and persistence of ecological systems. *Ecol. Lett.*, 4,
544   215–220.

545 Healy, K., Ezard, T.H.G., Jones, O.R., Salguero-Gómez, R. & Buckley, Y.M. (2019). Animal
546   life history is shaped by the pace of life and the distribution of age-specific mortality and
547   reproduction. *Nat. Ecol. Evol.*, 3, 1217–1224.

548 Higgins, S.I., Pickett, S.T.A. & Bond, W.J. (2000). Predicting extinction risks for plants:
549   Environmental stochasticity can save declining populations. *Trends Ecol. Evol.*

550 Hilde, C.H., Gamelon, M., Sæther, B.E., Gaillard, J.M., Yoccoz, N.G. & Pélabon, C. (2020).
551   The Demographic Buffering Hypothesis: Evidence and Challenges. *Trends Ecol. Evol.*,
552   35, 523–538.

553 Hoffmann, A.A. & Bridle, J. (2022). Plasticity and the costs of incorrect responses. *Trends
554   Ecol. Evol.*

555 Jackson, J., Le Coeur, C. & Jones, O. (2022). Life-history predicts global population
556   responses to the weather in the terrestrial mammals. *Elife*, 11.

557 Jensen, J.L.W.V. (1906). Sur les fonctions convexes et les inégalités entre les valeurs
558   moyennes. *Acta Math.*

559 Jones, O.R., Scheuerlein, A., Salguero-Gómez, R., Camarda, C.G., Schaible, R., Casper,
560   B.B., *et al.* (2014). Diversity of ageing across the tree of life. *Nature*, 505, 169–173.

561 Jongejans, E., de Kroon, H., Tuljapurkar, S. & Shea, K. (2010). Plant populations track rather
562   than buffer climate fluctuations. *Ecol. Lett.*, 13, 736–743.

563 King, J.G. & Hadfield, J.D. (2019). The evolution of phenotypic plasticity when
564   environments fluctuate in time and space. *Evol. Lett.*, 3, 15–27.

565 Klinkhammer, P.G.L. & de Jong, T.J. (1983). Is it profitable for biennials to live longer than
566   two years. *Ecol. Modell.*, 20, 223–232.

567 Knutson, T.R., McBride, J.L., Chan, J., Emanuel, K., Holland, G., Landsea, C., *et al.* (2010).

568   Tropical cyclones and climate change. *Nat. Geosci.*, 3, 157–163.

569 Koons, D.N., Pavard, S., Baudisch, A. & Jessica, C. (2009). Is life-history buffering or
570   lability adaptive in stochastic environments? *Oikos*, 118, 972–980.

571 Lande, R., Sæther, B.E. & Engen, S. (1997). Threshold harvesting for sustainability of
572   fluctuating resources. *Ecology*, 78, 1341–1350.

573 Lefkovitch, L.P. (1965). The Study of Population Growth in Organisms Grouped by Stages.
574   *Biometrics*, 21, 1–18.

575 Lennartsson, T. & Oostermeijer, J.G.B. (2001). Demographic variation and population
576   viability in Gentianella campestris: Effects of grassland management and environmental
577   stochasticity. *J. Ecol.*, 89, 451–463.

578 Leslie, P.H. (1945). On the Use of Matrices in Certain Population. *Biometrika*, 33, 183–212.

579 Levin, S.C., Evers, S., Potter, T., Guerrero, M.P., Childs, D.Z., Compagnoni, A., *et al.*
580   (2022). Rpadrino: An R package to access and use PADRINO , an open access database
581   of Integral Projection Models . *Methods Ecol. Evol.*, 2022, 1–7.

582 Mack, R.N. (2000). Cultivation fosters plant naturalization by reducing environmental
583   stochasticity. *Biol. Invasions*, 2, 111–122.

584 Marques, G.M., Augustine, S., Lika, K., Pecquerie, L., Domingos, T. & Kooijman, S.A.L.M.
585   (2018). The AmP project: Comparing species on the basis of dynamic energy budget
586   parameters. *PLoS Comput. Biol.*

587 Masson-Delmotte, V., Zhai, P., Pirani, A., Connors, S.L., Péan, C., Berger, S., *et al.* (2021).
588   IPCC: Climate Change 2021: The Physical Science Basis. *Cambridge Univ. Press.*
589   *Press.*

590 May, R.M. (1973). Stability in randomly fluctuating versus deterministic environments. *Am.*
591   *Nat.*, 107, 621–650.

592 McDonald, J.L., Franco, M., Townley, S., Ezard, T.H.G., Jelbert, K. & Hodgson, D.J. (2017).
593   Divergent demographic strategies of plants in variable environments. *Nat. Ecol. Evol.*, 1.

594 McDonald, J.L., Stott, I., Townley, S. & Hodgson, D.J. (2016). Transients drive the
595   demographic dynamics of plant populations in variable environments. *J. Ecol.*, 104,
596   306–314.

597 Melbourne, B.A. & Hastings, A. (2008). Extinction risk depends strongly on factors
598   contributing to stochasticity. *Nature*, 454, 100–103.

599 Merow, C., Bois, S.T., Allen, J.M., Xie, Y. & Silander, J.A. (2017). Climate change both
600   facilitates and inhibits invasive plant ranges in New England. *Proc. Natl. Acad. Sci. U.*
601   *S. A.*, 114, E3276–E3284.

602 Morris, W.F. & Doak, D.F. (2004). Buffering of Life Histories against Environmental
603   Stochasticity: Accounting for a Spurious Correlation between the Variabilities of Vital
604   Rates and Their Contributions to Fitness. *Am. Nat.*, 163, 579–590.

605 Morris, W.F., Pfister, C.A., Tuljapurkar, S., Haridas, C. V., Boggs, C.L., Boyce, M.S., *et al.*
606   (2008). Longevity can buffer plant and animal populations against chnaging climatic
607   variability. *Ecology*, 89, 19–25.

608 Neubert, M.G. & Caswell, H. (1997). Alternatives to resilience for measuring the responses
609   of ecological systems to perturbations. *Ecology*, 78, 653–665.

610 Nisbet, R.M., Muller, E.B., Lika, K. & Kooijman, S.A.L.M. (2000). From molecules to
611   ecosystems through dynamic energy budget models. *J. Anim. Ecol.*, 69, 913–926.

612 Orzack, S.H. (1985). Population dynamics in variable environments. V. The genetics of
613   homeostasis revisited. *Am. Nat.*, 125, 550–572.

614 Orzack, S.H. & Tuljapurkar, S. (1989). Population dynamics in variable environments. VII.
615   The demography and evolution of iteroparity. *Am. Nat.*, 133, 901–923.

616 Paniw, M., Ozgul, A. & Salguero-Gómez, R. (2018). Interactive life-history traits predict
617   sensitivity of plants and animals to temporal autocorrelation. *Ecol. Lett.*, 21, 275–286.

618 Petchey, O.L. (2000). Environmental colour affects aspects of single-species population
619   dynamics. *Proc. R. Soc. B Biol. Sci.*, 267, 747–754.

620 Petchey, O.L., Gonzalez, A. & Wilson, H.B. (1997). Effects on population persistence: the
621   interaction between environmental noise colour, intraspecific competition and space.
622   *Proc. R. Soc. London - Biol. Sci.*, 264, 1841–1847.

623 Pfister, C.A. (1998). Patterns of variance in stage-structured populations: Evolutionary
624   predictions and ecological implications. *Proc. Natl. Acad. Sci. U. S. A.*, 95, 213–218.

625 Revell, L.J. (2012). phytools: An R package for phylogenetic comparative biology (and other
626   things). *Methods Ecol. Evol.*, 3, 217–223.

627 Roerdink, J.B.T.M. (1988). The biennial life strategy in a random environment. *J. Math.
628   Biol.*, 26, 199–215.

629 Roerdink, J.B.T.M. (1989). The biennial life strategy in a random environment: Supplement.
630   *J. Math. Biol.*, 27, 309–319.

631 Romeijn, J. & Smallegange, I.M. (2022). Exploring how the fast-slow pace of life continuum
632   and reproductive strategies structure microorganism life history variation. *bioRxiv*.

633 de Roos, A.M. (1997). A gentle introduction to physiologically structured population models.
634   In: *Structured-population models in marine, terrestrial, and freshwater systems*. pp.
635   119–204.

636 de Roos, A.M. (2021). Dynamic population stage structure due to juvenile – adult asymmetry
637   stabilizes complex ecological communities. *Proc. Natl. Acad. Sci.*, 118.

638 de Roos, A.M., Metz, J.A.J., Evers, E. & Leipoldt, A. (1990). A size dependent predator-prey
639   interaction: who pursues whom? *J. Math. Biol.*, 28, 609–643.

640 Sæther, B.E., Coulson, T., Grøtan, V., Engen, S., Altwegg, R., Armitage, K.B., *et al.* (2013).
641   How life history influences population dynamics in fluctuating environments. *Am. Nat.*,
642   182, 743–759.

643 Saether, Engen, Islam, McCleery & Perrins. (1998). Environmental Stochasticity and
644   Extinction Risk in a Population of a Small Songbird, the Great Tit. *Am. Nat.*

645 Salguero-Gómez, R., Jones, O.R., Archer, C.R., Bein, C., de Buhr, H., Farack, C., *et al.*
646   (2016). COMADRE: A global data base of animal demography. *J. Anim. Ecol.*, 85, 371–
647   384.

648   Salguero-Gómez, R., Jones, O.R., Archer, C.R., Buckley, Y.M., Che-Castaldo, J., Caswell,
649   H., *et al.* (2015). The compadre Plant Matrix Database: An open online repository for
650   plant demography. *J. Ecol.*, 103, 202–218.

651   Salguero-Gómez, R., Jones, O.R., Blomberg, S.P., Hodgson, D.J., Zuidema, P.A. & Kroon,
652   H. De. (2017). Erratum: Fast–slow continuum and reproductive strategies structure plant
653   life-history variation worldwide (Proc Natl Acad Sci USA (2015) 113 (230–235) DOI:
654   10.1073/pnas.1506215112). *Proc. Natl. Acad. Sci. U. S. A.*, 114, E9753.

655   Santos, G.S., Gascoigne, S.J.L., Dias, A.T.C., Kajin, M. & Salguero-Gómez, R. (2023). A
656   unified framework to identify demographic buffering in natural populations. *bioRxiv*, 1–
657   31.

658   Sheth, S.N. & Angert, A.L. (2018). Demographic compensation does not rescue populations
659   at a trailing range edge. *Proc. Natl. Acad. Sci. U. S. A.*, 115, 2413–2418.

660   Smallegange, I.M., Caswell, H., Toorians, M.E.M. & de Roos, A.M. (2017). Mechanistic
661   description of population dynamics using dynamic energy budget theory incorporated
662   into integral projection models. *Methods Ecol. Evol.*

663   Smallegange, I.M., Deere, J.A. & Coulson, T. (2014). Correlative changes in life-history
664   variables in response to environmental change in a model organism. *Am. Nat.*, 183, 784–
665   797.

666   Stott, I, Townley, S. & Hodgson, D.J. (2011). A framework for studying transient dynamics
667   of population projection matrix models. *Ecol. Lett.*, 14, 959–970.

668   Sutherland, W.J., Freckleton, R.P., Godfray, H.C.J., Beissinger, S.R., Benton, T., Cameron,
669   D.D., *et al.* (2013). Identification of 100 fundamental ecological questions. *J. Ecol.*, 101,
670   58–67.

671   Trenberth, K.E. (2011). Changes in precipitation with climate change. *Clim. Res.*, 47, 123–
672   138.

673   Tuljapurkar, S. (1982). Population dynamics in variable environments. III. Evolutionary
674   dynamics of r-selection. *Theor. Popul. Biol.*, 21, 141–165.

675   Tuljapurkar, S. (1989). An uncertain life: Demography in random environments. *Theor.*
676   *Popul. Biol.*, 35, 227–294.

677   Tuljapurkar, S., Gaillard, J.M. & Coulson, T. (2009). From stochastic environments to life
678   histories and back. *Philos. Trans. R. Soc. B Biol. Sci.*, 364, 1499–1509.

679   Tuljapurkar, S. & Haridas, C. V. (2006). Temporal autocorrelation and stochastic population
680   growth. *Ecol. Lett.*, 9, 327–337.

681   Tuljapurkar, S., Horvitz, C.C. & Pascarella, J.B. (2003). The Many Growth Rates and
682   Elasticities of Populations in Random Environments. *Am. Nat.*, 162.

683   Tuljapurkar, S. & Istock, C. (1993). Environmental uncertainty and variable diapause. *Theor.*
684   *Popul. Biol.*

685   Tuljapurkar, S. & Lee, R. (1997). Demographic uncertainty and the stable equivalent
686   population. *Math. Comput. Model.*, 26, 39–56.

687   Urban, M.C. (2015). Accelerating extinction risk from climate change. *Science (80-.).*, 348,
688   571–573.

689 Varas-Enriquez, P.J., van Daalen, S. & Caswell, H. (2022). Individual stochasticity in the life
690   history strategies of animals and plants. *bioRxiv*.

691 Vinton, A.C., Gascoigne, S.J.L., Sepil, I. & Salguero-Gómez, R. (2022). Plasticity's role in
692   adaptive evolution depends on environmental change components. *Trends Ecol. Evol.*,
693   37, 1067–1078.

694 Vinton, A.C., Gascoigne, S.J.L., Sepil, I. & Salguero-Gómez, R. (2023). The importance of
695   spatial and temporal structure in determining the interplay between plasticity and
696   evolution. *Trends Ecol. Evol.*, 38, 221–223.

697 Wang, J., Yang, X., Silva Santos, G., Ning, H., Li, T., Zhao, W., *et al.* (2023). Flexible
698   demographic strategies promote the population persistence of a pioneer conifer tree
699   (Pinus massoniana) in ecological restoration. *For. Ecol. Manage.*, 529, 120727.

700 Westerband, A.C. & Horvitz, C.C. (2017). Photosynthetic rates influence the population
701   dynamics of understory herbs in stochastic light environments. *Ecology*, 98, 370–381.

702 Wieczynski, D.J., Turner, P.E. & Vasseur, D.A. (2018). Temporally autocorrelated
703   environmental fluctuations inhibit the evolution of stress tolerance. *Am. Nat.*, 191,
704   E195–E207.

705 Wiener, P. & Tuljapurkar, S. (1994). Migration in variable environments: Exploring life-
706   history evolution using structured population models. *J. Theor. Biol.*, 166, 75–90.

707

708

709

710

711

712

713

714

715

716

717

718

719 FIGURES

720

Figure 1. An overview of the simulation and analysis structure implemented to examine the impacts of climate drivers on natural populations. In our simulations, we explored how a population's measure of demographic buffering changes over the parameter space of possible environment autocorrelation and variance values. (a) This space is visualized here across a 2D surface with environment autocorrelation on the x-axis and proportional variance on the y-axis. Environment variance is noted as proportional variance which is defined as the relative increase (>1) or decrease (<1) in the variance of a climate driver is made relative to the climate driver's variance value stored in the PADRINO database. The middle of this landscape (*i.e.*, autocorrelation $= 0$ and proportional variance $= 1$) represents the population model stored in the PADRINO database. (b) The impact of environment autocorrelation and variance on a response variable (*e.g.*, degree of demographic buffering or a measure of population structure) is shown projected as a third dimension across this landscape. Across this projection, values lower than those reported in the original PADRINO IPM model are coloured purple, values close to the PADRINO model are coloured white, and values greater than the PADRINO model are coloured green. (c) The most parsimonious model that predicts the response variable as a function of environment autocorrelation and proportional variance

737 was retained to calculate the summed linear and non-linear contribution of each predictor and

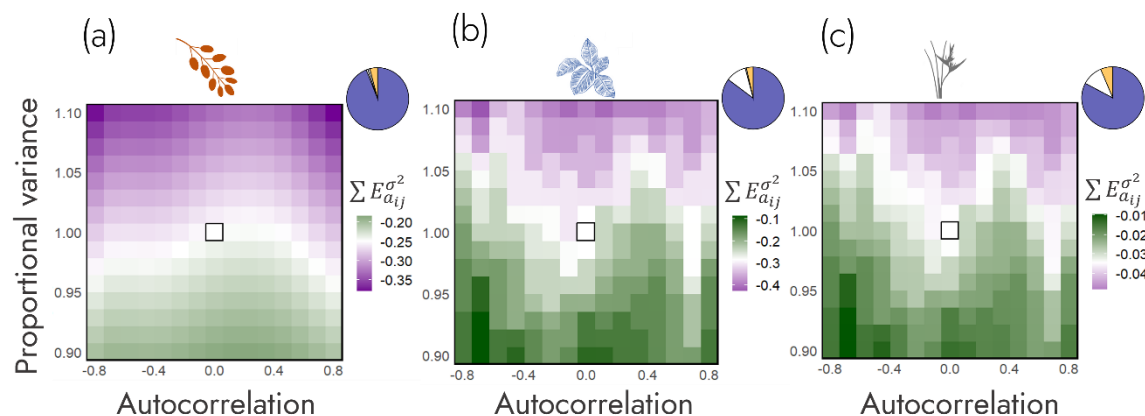738 the residuals towards the variance in the response variable.

739

740

741

742

Figure 2. Environment variance (σ^2) is the primary driver of demographic buffering. Across *Berberis thunbergii* (a), *Calathea crotalifera* (b) and *Heliconia tortuosa* (c), environment variance (blue in pie-chart) explains the majority of variance in $\sum E_{a_{ij}}^{\sigma^2}$. Populations of all three species become relatively less buffered (lower values of $\sum E_{a_{ij}}^{\sigma^2}$, in purple) as proportional variance of environment components increase, whilst populations become relatively more buffered (higher values of $\sum E_{a_{ij}}^{\sigma^2}$, in green) as environment variance decreases. This strong impact of proportional variance of environment components is summarized in the pie charts detailing the proportion of variance in $\sum E_{a_{ij}}^{\sigma^2}$ that can be explain by the environment components: environment autocorrelation in orange, environment variance in blue, environment autocorrelation × variance interaction in grey (so small here it is not visible), and unexplained residuals in white. Since the pie charts are predominantly blue across all three species, variance in environment components is the primary driver of $\sum E_{a_{ij}}^{\sigma^2}$ across the environment autocorrelation – variance parameter space.
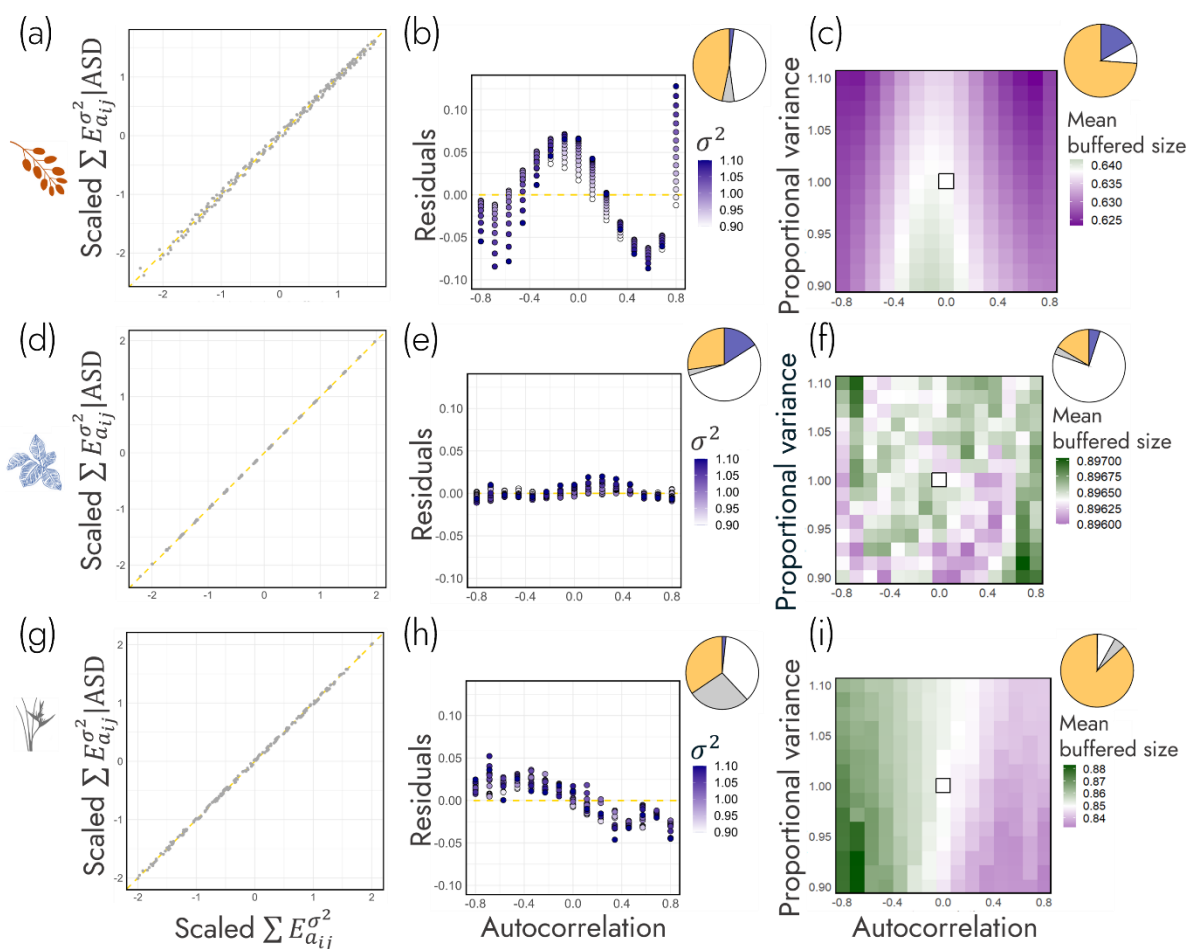
756

Figure 3. Environment autocorrelation can influence demographic buffering ($\sum E_{a_{ij}}^{\sigma^2}$) via its

impact on population structure. In addition, the degree to which environmental

autocorrelation impacts $\sum E_{a_{ij}}^{\sigma^2}$ across *Berberis thunbergii* (a-c), *Calathea crotalifera* (d-f) and

Heliconia tortuosa (g-i) is species-specific. The first column (a, d, g) shows the correlation

between $\sum E_{a_{ij}}^{\sigma^2}$ and demographic buffering weighted by the average stage distribution

($\sum E_{a_{ij}}^{\sigma^2}$ |ASD). Residuals from these regressions show the potential impact of population

structure on $\sum E_{a_{ij}}^{\sigma^2}$. We then, in the second column (b, e, h), investigate these residuals as a

function of the environment autocorrelation (x-axis) and environmental variance (σ^2; purple).

Lastly, in the third column (c, f, i), we quantify the impact of environment autocorrelation

and variance on the mean buffered size of the population. The pie charts at the top right-hand

767   corner of panels in (b, e, h), and (c, f, i) detail the proportion of variance in $\sum E_{a_{ij}}^{\sigma^2}$ that is

768   explained by environment autocorrelation (orange), environment variance (blue),

769   environment autocorrelation $\times$ variance interaction (grey) and residuals (white). These pie

770   charts show how environmental autocorrelation is the primary driver of shifts in $\sum E_{a_{ij}}^{\sigma^2}$ due to
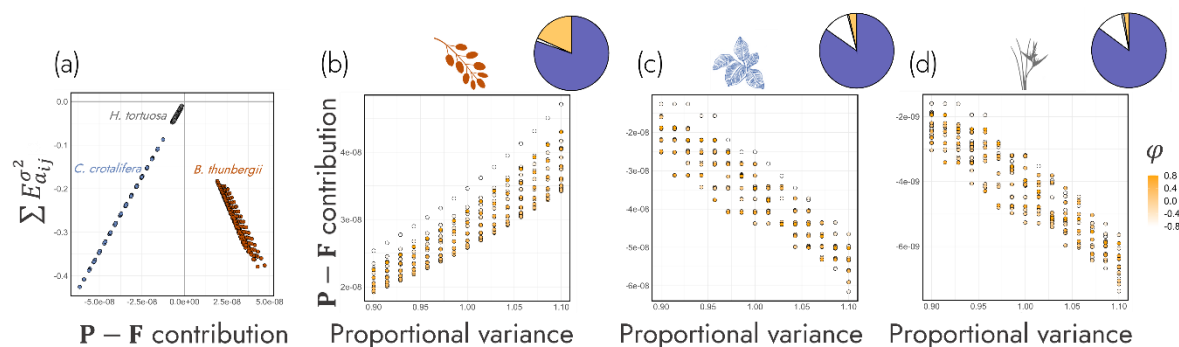
771   population.

772

773

Figure 4. Environment variance (σ^2) influences demographic buffering ($\sum E_{a_{ij}}^{\sigma^2}$) via the population's underlying demographic rates. (a) The relative contribution of progression (growth conditional on survival: **P**) and fertility (recruitment of new individuals from reproductive ones the previous year: **F**) on $\sum E_{a_{ij}}^{\sigma^2}$ (*i.e.*, **P-F** contribution). This approach was then applied to three plant species: (b) *Berberis thunbergii*, (c) *Calathea crotalifera*, and (d) *Heliconia tortuosa*). Dots are coloured by the degree of environment autocorrelation (yellow). The pie charts at the top right-hand corner of panels b-d detail the proportion of variance in $\sum E_{a_{ij}}^{\sigma^2}$ that is explained by environment autocorrelation (φ, orange), environment variance (blue), environment autocorrelation × variance interaction (grey) and residuals (white). These pie charts show how environment variance is the primary driver of shifts in the relative contributions of progression and fertility to $\sum E_{a_{ij}}^{\sigma^2}$.